IEICE TRANS. ELECTRON , VOL.E86–C, NO.11 NOVEMBER 2003

PAPER Special Issue on Analytical and Simulation Methods for Electromagnetic Wave Problems

FEM-Based Electromagnetic Wave Simulator Running on Some Platforms by Use of Java and a Commercial Tool

Koichi HIRAYAMA[†a)], *Regular Member*, **Naoto KUNIEDA**[†], *Student Member*, **Yoshio HAYASHI**[†], *Regular Member*, *and* **Masanori KOSHIBA**[††], *Fellow*

SUMMARY Making up an electromagnetic wave simulator based on the FEM is tried, which may run on some widely used platforms by use of Java and a single commercial tool. Since the codes and configuration files to be created for this simulator are common, one can construct the simulator running on the platforms at the same time. Using this simulator, the transmission properties of two- and three-dimensional waveguide discontinuities in optical and microwave waveguides are analyzed, the inverse problem in material constant measurement is solved, and the computed results are presented including plots of the electric field distribution.

key words: *electromagnetic wave simulator, FEM, Java, anisotropic PML, waveguide discontinuity, inverse problem*

1. Introduction

A number of researchers engaged in numerical analysis have intensively developed solvers based on their novel formulations, but most of them, especially in universities, have not paid much attention in making up a simulator with a pre- and postprocessor for their solvers. Although some of their solvers may be applicable to various types of microwave and optical waveguides with complicated geometry, the researchers may not be able to make the best use of them since it is difficult or impossible to give geometry data in text style. Also, the visualization of numerical results in postprocessing plays an important role in the knowledge of the physical meaning of the results and the design of a waveguide. On the other hand, it is a difficult task for researchers to construct a simulator with a pre- and postprocessor of a graphical user interface (GUI), because they are required to have knowledge of the programming on a particular window system of a platform (Windows [1], Unix, Linux, etc.). Also, a mesh generator, a software tool which divides a surface or volume into a number of small subdomains automatically, should be involved in a preprocessor for some solvers, especially those based on the finite-element method (FEM).

Recently, we constructed a microwave simulator which has analysis methods based on the FEM as solvers and two commercial tools as a pre- and postprocessor of a GUI [2]. However, this simulator can run on Windows only, and needs two commercial tools.

In this paper, we try to make up an electromagnetic wave simulator based on the FEM, which may run on some widely used platforms and needs a single commercial tool. The FEM has an advantage that it is easily applicable to the analysis of a waveguide including a curved structure. This simulator is, to the best of our knowledge, the first one having the main user interface made by use of Java [3]. A commercial tool, GiD [4], is used as a GUI tool both for the input of geometry data in preprocessing and for the output of an electromagnetic field distribution in postprocessing. To construct such a simulator, one must create the source codes of a solver and Java, some configuration files for the data format in GiD, but, fortunately, since their codes and files are common on Windows, Linux, and Solaris, one can construct the simulator running on the three platforms at the same time. At this point, we paid attention to the fact that the screen made by Java may be displayed with a little difference in the size and configuration of some objects (labels, text boxes, etc.) on each of their platforms. Also, the interconnection between Java and GiD or solvers is made via text files to run this simulator readily on the platforms.

The rest of the paper is organized as follows. In Sect. 2, the solvers for a discontinuity region of an open structure are formulated. In Sect. 3, the analysis of the transmission properties of three-dimensional waveguide discontinuities in a microwave waveguide is described to demonstrate this simulator in detail and confirm the usefulness of the solver in Sect. 2.2. In Sect. 4, the material constant measurement is analyzed to confirm the usefulness of the solver with the perfectly matched layer (PML) [5] in Sect. 2.2, and this section illustrates that it is an advantage of this simulator to be able to easily incorporate such a particular solver for the inverse problem. Also, we show that loading the PML is valid to suppress unnecessary reflection and improve the accuracy in the estimation of material constants. In Sect. 5, the transmission properties of a two-dimensional waveguide discontinuity in an optical waveguide is computed to confirm the usefulness of the solver in Sect. 2.1. Finally, Sect. 6 concludes the paper.

Manuscript received March 24, 2003.
Manuscript revised May 12, 2003.

[†]The authors are with the Depertment of Electrical and Electronic Engineering, Kitami Institute of Technology, Kitami-shi, 090-8507 Japan.

[††]The author is with the Division of Electronics and Information Engineering, Hokkaido University, Sapporo-shi, 060-8628 Japan.

a) E-mail: hirakc@mail.kitami-it.ac.jp

2. Finite Element Formulation

Some solvers in our simulator are described in [2], and at present we add a couple of solvers based on the following formulation so that we may treat a discontinuity region of an open structure by loading the anisotropic PML [5].

2.1 2-D Optical Waveguide Discontinuity

We consider a two-dimensional optical waveguide discontinuity problem, as shown in Fig. 1, where boundary Γ_0 is perfect conductor, and boundary Γ_i $(i = 1, 2, \cdots, N)$ connects the discontinuity region Ω to the uniform 3-layer slab waveguide i, and the anisotropic PML [5] is loaded between Ω and Γ_0 to analyze an open waveguide discontinuity problem. Assuming that there is no variation of fields and refractive indices in the z direction, we can obtain the following equation with respect to $\phi = E_z$ (E_z being the z component of the electric field):

$$\frac{\partial}{\partial x}\left(\frac{s_y}{s_x}\frac{\partial \phi}{\partial x}\right) + \frac{\partial}{\partial y}\left(\frac{s_x}{s_y}\frac{\partial \phi}{\partial y}\right) + k_0^2 n^2 s_x s_y \phi = 0 \quad (1)$$

where k_0 is a wavenumber in vacuum, and n represents a refractive index of material. The value of the PML parameter s_w $(w = x, y)$ is unity in Ω and is given in a PML region as follows:

$$s_w = 1 - j\frac{-3\ln|R|}{2k_0 n d_w^3}(w - w_0)^2 \quad (2)$$

where d_w is the thickness of the PML in the w direction, w_0 stands for the w coordinate at the beginning of the PML, and $|R|$ is a constant of small value. Also, $s_x = 1$ in PML(I) and $s_y = 1$ in PML(II).

Applying the Galerkin procedure to Eq. (1), we obtain

$$\iint_{\Omega_0}\left(\frac{s_y}{s_x}\frac{\partial \tilde{\phi}}{\partial x}\frac{\partial \phi}{\partial x} + \frac{s_x}{s_y}\frac{\partial \tilde{\phi}}{\partial y}\frac{\partial \phi}{\partial y} - k_0^2 n^2 s_x s_y \tilde{\phi}\phi\right)dxdy$$

$$= \int_\Gamma \tilde{\phi}\left(\frac{\partial \phi_{\Gamma-}^{\mathrm{inc}}}{\partial x_1} - \frac{\partial \phi_{\Gamma+}^{\mathrm{inc}}}{\partial x_1}\right)dy_1 \quad (3)$$

where $\tilde{\phi}$ is a test function, and Ω_0 stands for the sum region of Ω and the PML regions. Also, $\Gamma(= \Gamma_1)$ represents the incident plane, and $\phi_{\Gamma\pm}^{\mathrm{inc}}$ stands for the incident field at the $\pm x_1$ side of Γ and is given as follows [6]:

$$\phi_{\Gamma\pm}^{\mathrm{inc}} = f_{1m}(y_1)\exp(\mp \jmath \beta_{1m} x_1) \quad (4)$$

where f_{1m} and β_{1m} are the modal function and the propagation constant of the m-th guided mode in waveguide 1, respectively.

Dividing and discretizing Ω_0 by quadratic triangular elements, we obtain the following matrix equation:

$$\begin{bmatrix} [A_{00}] & [A_{0\Gamma}] \\ [A_{\Gamma 0}] & [A_{\Gamma\Gamma}] \end{bmatrix}\begin{bmatrix} \{\phi_0\} \\ \{\phi_\Gamma\} \end{bmatrix} = \begin{bmatrix} \{0\} \\ \{\psi_\Gamma\} \end{bmatrix} \quad (5)$$

where the components of vector $\{\phi_0\}$ are the values of ϕ in Ω_0 except on Γ and Γ_0, and those of $\{\phi_\Gamma\}$ are the values of ϕ on Γ. Also, $[A_{00}], [A_{0\Gamma}], [A_{\Gamma 0}]$, and $[A_{\Gamma\Gamma}]$ are finite-element matrices, and $\{\psi_\Gamma\}$ corresponds to the incident field. Since the right-hand side of Eq. (5) has a sparse and complex matrix, the final matrix equation can be solved efficiently with much reduction of computational time and memory.

2.2 3-D Waveguide Discontinuity

We consider a three-dimensional microwave waveguide discontinuity, as shown in Fig. 2, where boundary Γ_0 is perfect conductor, and boundary Γ_i $(i = 1, 2, \cdots, N)$ connects the discontinuity region Ω to the uniform waveguide i surrounded by perfect conductor. If necessary, the anisotropic PML [5] is loaded at the border of Ω, but at present the uniform waveguides are limited to be shielded by perfect conductor in this simulator. We can obtain the following vector wave function with respect to the electric field $\boldsymbol{E}$:

$$\nabla \times \left(\frac{1}{\mu_r}[s]^{-1}\nabla \times \boldsymbol{E}\right) - k_0^2 \varepsilon_r [s]\boldsymbol{E} = 0 \quad (6)$$

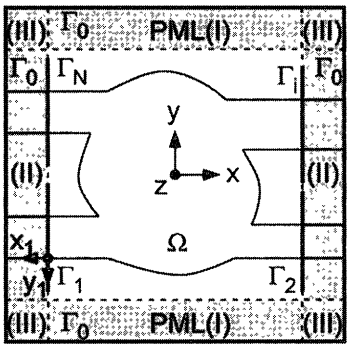

Fig. 1 2-D optical waveguide discontinuity.

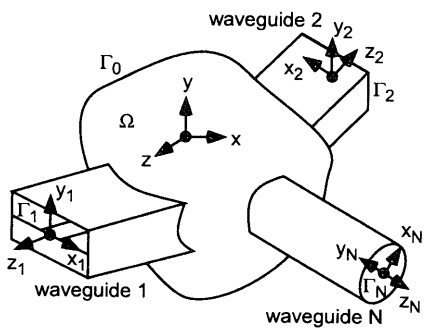

Fig. 2 3-D microwave waveguide discontinuity.

where ε_r and μ_r are the relative permittivity and permeability, respectively. The matrix $[s]$ of the PML is given as follows:

$$[s] = \begin{bmatrix} s_y s_z / s_x & 0 & 0 \\ 0 & s_z s_x / s_y & 0 \\ 0 & 0 & s_x s_y / s_z \end{bmatrix} \tag{7}$$

where the value of s_w $(w = x, y, z)$ in a PML region is given in Eq. (2). We can obtain the following functional with respect to the electric field $\boldsymbol{E}$:

$$\begin{aligned} F(\boldsymbol{E}) = \frac{1}{2} \iiint_{\Omega} \Big[(\nabla \times \boldsymbol{E}) \cdot \left(\frac{1}{\mu_r} [s]^{-1} \nabla \times \boldsymbol{E} \right) \\ - k_0^2 \varepsilon_r \boldsymbol{E} \cdot [s] \boldsymbol{E} \Big] dx dy dz \\ + \frac{1}{2} \sum_{i=1}^{N} \iint_{\Gamma_i} \boldsymbol{E}_i \cdot \boldsymbol{P}_i(\boldsymbol{E}_i)\, dx_i dy_i \\ - \iint_{\Gamma_1} \boldsymbol{E}_1 \cdot \boldsymbol{Q}\, dx_1 dy_1 \end{aligned} \tag{8}$$

where $\boldsymbol{E}_i$ denotes $\boldsymbol{E}$ on Γ_i. Here the uniform waveguides are formulated based on the eigenmode expansion, and the eigenmodes are calculated numerically using the FEM, because eigenmodes of uniform waveguides may not be expressed analytically. The symbol $\boldsymbol{P}_i(\boldsymbol{E}_i)$ is expressed with the propagation constants and the modal function of the eigenmodes in waveguide i, and $\boldsymbol{Q}$ denotes an incident wave from waveguide 1.

Applying the variational principle to Eq. (8), dividing and discretizing region Ω by tetrahedral edge elements, we obtain the following matrix equation:

$$[A]\{\phi\} + \sum_{i=1}^{N} [P_i]\{\phi_i\} = \{Q\} \tag{9}$$

where the components of vector $\{\phi\}$ are the values of the electric field at the sides of the elements in Ω except on perfect conductor, and the components of vector $\{\phi_i\}$ are the values on Γ_i. Since the right-hand side of Eq. (9) has a sparse and complex matrix, the final matrix equation can be solved efficiently with much reduction of computational time and memory.

3. Coupled Microstrip Lines via a Slot

We consider the coupling problem of two microstrip lines via a slot in a common ground plane, as shown in Fig. 3, where the lines and the ground plane are made of perfect conductor, and the thickness of the lines is infinitesimal. The width of microstrip lines 1 and 2 is 2.54 mm, and the thickness and the relative permittivity of substrates 1 and 2 are 0.762 mm and 2.17, respectively, and the size of the shielding waveguide is $W = 50$ mm and $H_1 = H_2 = 50$ mm. Also, two slots are shown in Fig. 4, where the slot size is $a = 5.3$ mm and $b = 14.96$ mm in the rectangular slot, and $a = 1.256$ mm and $b = 15.159$ mm in the elliptical one [7]. Only a half region is analyzed for the symmetry of the structure.

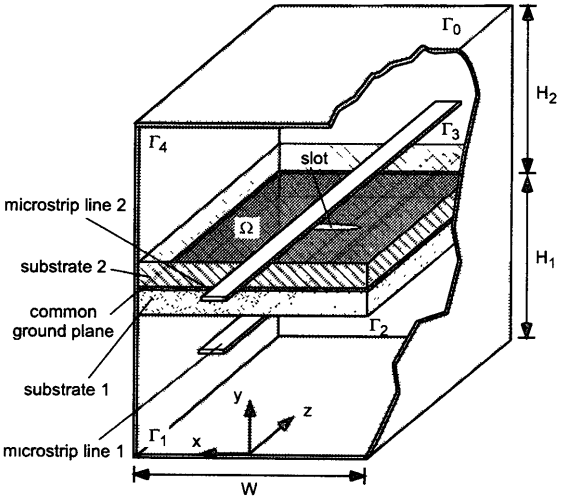

Fig. 3 Coupled microstrip lines via a slot.

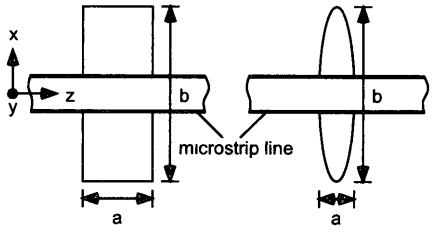

Fig. 4 Rectangular and elliptical slots (top view).

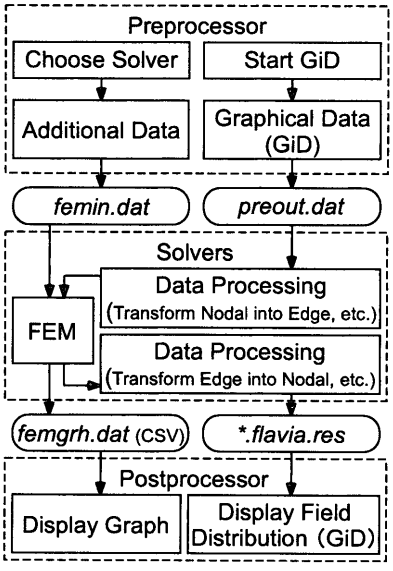

Fig. 5 Structure of simulator (FEMSKiT).

3.1 Outline of Simulator

Figure 5 shows the structure of our simulator named FEMSKiT (Finite-Element ElectroMagnetic-wave Sim-

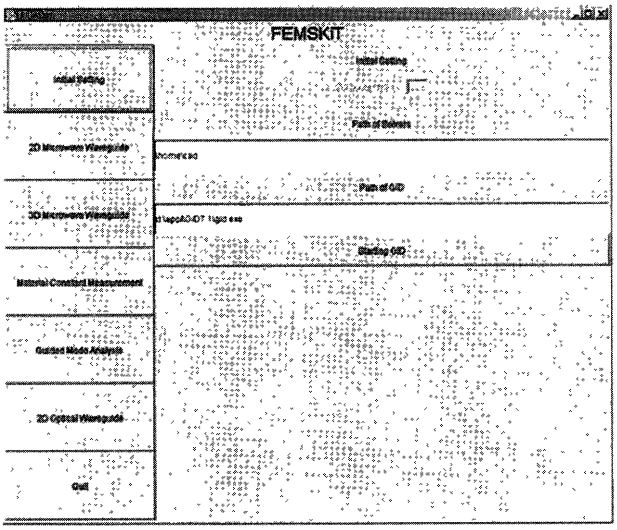

Fig. 6 Screen for the specification of the paths of the solvers and GiD

ulator at Kitami Institute of Technology), where an oval box stands for a text file, the processings of two rectangular boxes with '(GiD)' are run on a commercial tool, GiD, the solvers are coded in FORTRAN, and the others are made up in Java.

3.2 Preprocessing

There are a number of commercial or public-domain tools which can define various types of geometry of microwave and optical waveguides and then divide a surface into triangular elements in a 2-D waveguide or a volume into tetrahedral elements in a 3-D waveguide. Some of the tools are available via the Internet and free of charge (in a limited period or function). We decided to use GiD [4], because GiD can define geometry through a GUI and be run on several platforms including Windows, Linux, and Solaris.

Figure 6 shows the screen which appears after starting our simulator. First we must give the paths of the solvers and GiD, because the paths may be different in each of the computers into which the simulator are installed. Next we start GiD, and then draw the waveguide structure, give the boundary condition, specify the surfaces corresponding to the input/output ports and so on by using the GUI in GiD. Figure 7 shows a screen after inputting the structure of the coupled microstrip lines via an elliptical slot. Dividing the computational region into a number of tetrahedral elements by using a mesh generator involved in GiD, we save the data, including the nodal points of the elements and their coordinates, in a file *preout.dat*.

Next, when choosing one of the solvers listed in the left row of the screen of our simulator, another screen appears for the input of the additional data. Figure 8 shows the screen for the additional data in

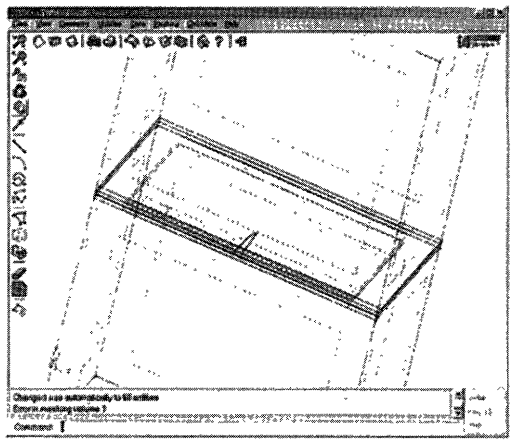

Fig. 7 Screen of the GUI in GiD

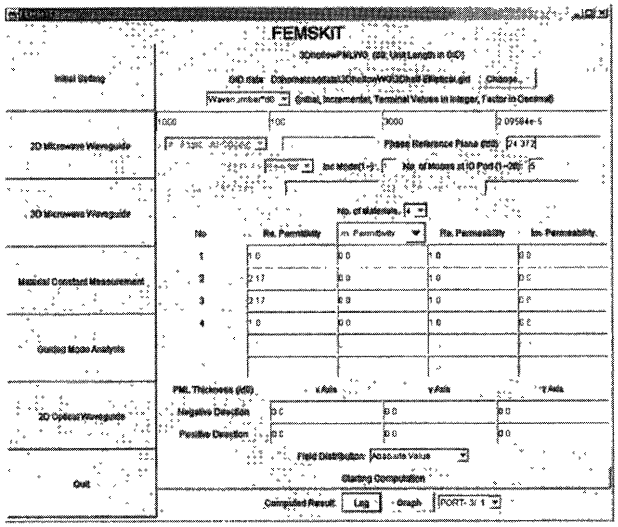

Fig. 8 Screen for the input of the additional data.

the 3-D microwave waveguide discontinuity. We specify the path of the GiD data, the wavenumber of the incident wave, the incident mode number, and the number of the eigenmodes taken into account in the eigenmode expansion of the uniform waveguides. Here the wavenumber may be given as a variable to compute the frequency characteristics of the S parameters. Also, we specify the number of the materials and their material constants. If the PML is loaded, its thickness must be given. Finally, we choose either the instantaneous or absolute value in plotting the electric field distribution in postprocessing.

3.3 Solver

When clicking the button 'Starting Computation,' the solver starts. At this time, the additional data given on the screen of Fig. 8 is saved in a file *femin.dat*, and the file as well as *preout.dat* are fed to the solver. Since GiD is mainly developed for the finite-element analysis

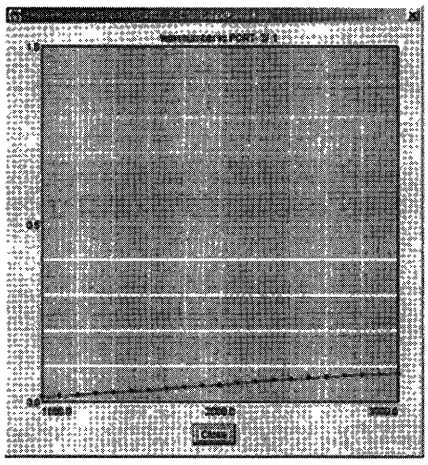

Fig. 9 Plot in Java of the transmission power at port 3 for the coupled microstrip lines via an elliptical slot versus frequency.

in the field of structural mechanics, only nodal elements are supported. However, since some solvers in our simulator use edge or edge/nodal elements to avoid spurious (non-physical) solutions, it is necessary to add the program which transforms the data of nodal elements generated by GiD into those of edge or edge/nodal elements.

The solvers create a file *femlog.txt* having the detailed computed results and a file *femgrh.dat* written in CSV (Comma Separated Value) format to display a graph of the reflection and transmission power versus wavenumber or wavelength in postprocessing. Since a file in CSV format may be fed to various tools which draw a graph, one can make a graph with good quality from *femgrh.dat*, if necessary. Also, to display the electric field distribution in postprocessing, the solvers create a file **.flavia.res* (* being the folder name in which the GiD data are saved) written in a format that GiD requires. The program which transforms the data of edge or edge/nodal elements into those of nodal elements must be incorporated into the solvers which use edge or edge/nodal elements.

3.4 Postprocessing

The detailed computed results and the graph of the reflection and transmission power may be displayed by clicking the button 'Log' and 'Graph,' respectively. We analyzed the coupled microstrip lines via a rectangular and elliptical slot for the fundamental mode incidence at port 1 on boundary Γ_1. Figure 9 plotted in Java shows the transmission power at port 3 on boundary Γ_3 for the coupling via an elliptical slot versus frequency. Also, Fig. 10 plotted in GiD shows the electric field distribution on the common ground plane in the neighborhood of the slots at 1 GHz. Here we specified finer element division along the circumference of the slots in GiD. It is much advantage of the FEM to be able to easily treat a structure of curved shape when compared to the FDTD.

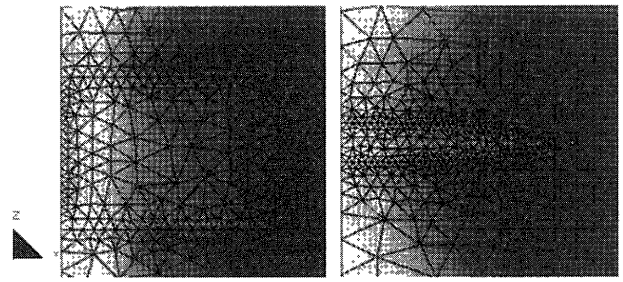

Fig. 10 Plot in GiD of the electric field distribution near a rectangular and elliptical slot

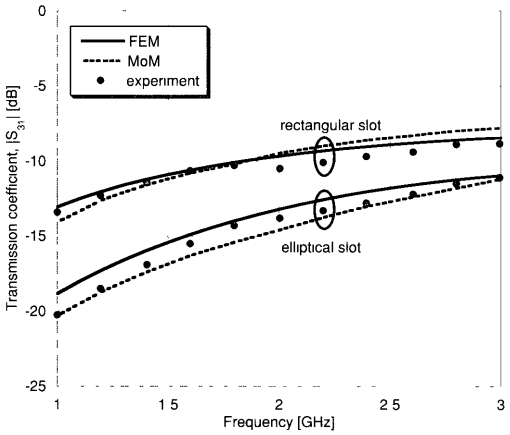

Fig. 11 Coupling between two microstrip lines via a slot

Figure 11, which is plotted with good quality in another commercial tool from *femgrh.dat*, shows the transmission coefficient at port 3 versus frequency. We find that the results of the FEM agree well with those of the method of moments (MoM) and the experiment in [7].

In the computation for the coupled microstrip lines via an elliptical slot, the number of the tetrahedral elements was 31825, the number of the unknowns in the final Eq. (9) was 36190, and the computational time on a computer with Intel Pentium 4 of 2.40 GHz and 1 Gbyte memory was about 4 minutes for a frequency.

4. Material Constant Measurement Using Flanged Rectangular Waveguides

We consider the simultaneous measurement of the permittivity and permeability of a lossy sheet using flanged rectangular waveguides, as shown in Fig. 12 [8]. In [8], the computation of S parameters, corresponding to the direct problem, was done by using the method of moments (MoM) and the FEM, while the estimation of the permittivity and permeability, corresponding to the inverse problem, was done by using the MoM only. At present, for the inverse problem, we have in our simulator a solver ('Material Constant Measurement' in Fig. 5) based on the FEM and the Newton method.

When compared to the MoM, the FEM has the advantage that it is possible to compute with a single solver both for the infinite and the finite size of the flange and/or the lossy sheet, if necessary, by loading the PML.

When assuming that the thickness and the cross section of a lossy sheet are 1.5 mm and a 30 mm × 30 mm square, respectively, the rectangular waveguide is WRJ-10 of $a = 22.9$ mm and $b = 10.2$ mm, and the frequency is 8.505 GHz, the material constants estimated using our simulator was $\varepsilon_r = 8.68 - j0.187$ and $\mu_r = 1.75 - j1.16$. Here the S parameters obtained from the direct problem for a 100 mm × 100 mm lossy sheet of $\varepsilon_r = 8.68 - j0.182$ and $\mu_r = 1.75 - j1.16$ was used as a substitute for measured ones, and only a quarter region was analyzed for the symmetry of the structure. Figure 13(a) shows the electric field distribution, and we find that the reflection arises from the perfect conductor of the side of the sheet in the y direction. To vanish this reflection, we loaded the PML of thickness 5 mm inside the sheet in the y direction. Then the estimated material constants were $\varepsilon_r = 8.68 - j0.184$ and $\mu = 1.75 - j1.16$, and the electric field distribution is shown in Fig. 13(b), where the reflection in the y direction is not observed.

In the inverse problem for a 30 mm × 30 mm lossy sheet inside which the PML is loaded, the Newton method converged for the fourth estimated value. In this computation, the number of the tetrahedral elements was 6663, the number of the unknowns in the final Eq. (9) was 7129, and the computational time on the same computer as in Sect. 3 was about 11 minutes.

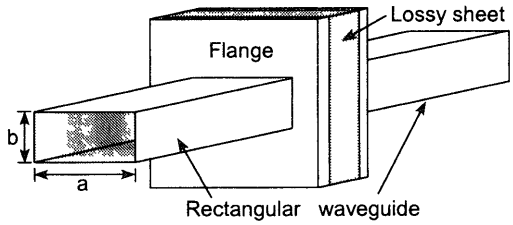

Fig. 12 Material constant measurement of a lossy sheet placed between flanged rectangular waveguides

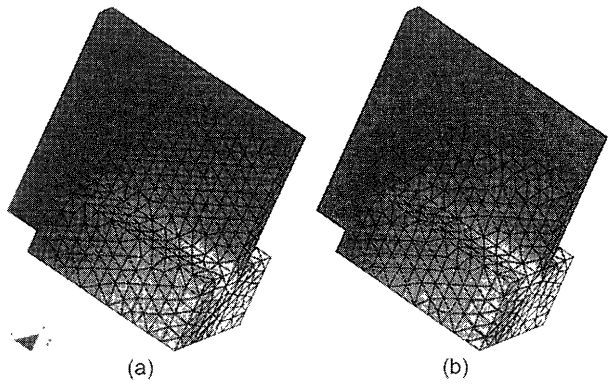

Fig. 13 Electric field distribution for the material constant measurement, where figures (a) and (b) are the computed results without and with the PML, respectively

5. Ring Resonator Filter

We consider a two-dimensional ring resonator filer, as shown in Fig. 14, where the inner radius and the width of the ring are $a = 1.6\,\mu$m and $d = 0.2\,\mu$m, the width of the waveguides is $w = 0.2\,\mu$m, the distance between the ring and the waveguides is $g = 0.2\,\mu$m, and the refractive indices are $n_0 = 1$ and $n_1 = 3$ [9]. Here the size of the computational region Ω_0 including the PML is $10\,\mu\text{m} \times 9\,\mu$m, and the thicknesses of the PML in the x and y directions are $2.5\,\mu$m and $0.5\,\mu$m, respectively. We analyzed this filter by using a solver ('2D Optical Waveguide' in Fig. 5) in our simulator for the fundamental TE mode incidence at port 1, and show in Fig. 15 the transmission power at port 4 versus wavelength. We find that the transmission power becomes almost unity at the resonant wavelength of the ring [10]. Also, the instantaneous electric field distribution is shown in Fig. 16 at the wavelength of 1.334 μm, which is nearly equal to one of the resonant wavelengths.

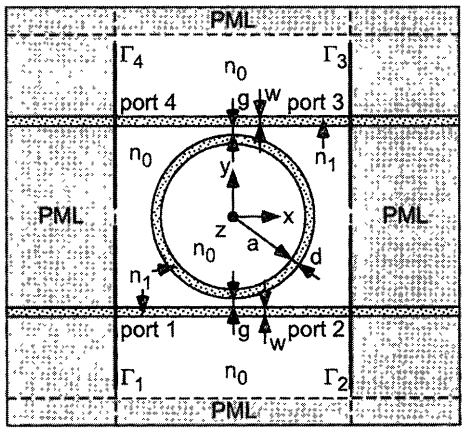

Fig. 14 Ring resonator filter

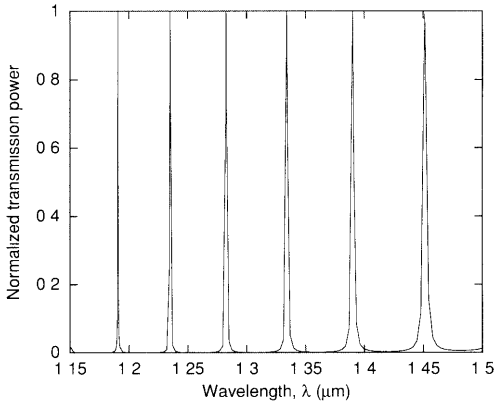

Fig. 15 Transmission power at port 4 of the ring resonator filter

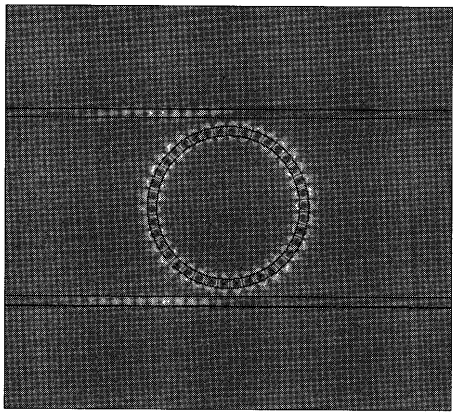

Fig. 16 Instantaneous electric field distribution in the ring resonator filter at the wavelength of 1.334 μm.

In this computation, the number of the quadratic triangular elements was 14140, the number of the unknowns in the final Eq. (5) was 28037, and the computational time on the same computer as in Sect. 3 was about 9 seconds for a wavelength.

6. Conclusion

We have made up an electromagnetic wave simulator based on the FEM which may run on Windows, Linux, and Solaris by use of Java and GiD. Since the codes and configuration files to be created for this simulator are common, one can construct the simulator running on the three platforms at the same time. Using this simulator, the transmission properties of two- and three-dimensional waveguide discontinuities in optical and microwave waveguides were analyzed, the inverse problem in material constant measurement was solved, and the computed results were compared with those of other numerical analysis methods and experiments to show the validity of our solvers.

References

[1] http://www.microsoft.com/japan/
[2] K. Hirayama, Y. Hayashi, and M. Koshiba, "Microwave simulator based on the finite-element method by use of commercial tools," IEICE Trans. Electron., vol.E84-C, no.7, pp.905–913, July 2001.
[3] http://jp sun.com/java/
[4] http://gid cimne.upc.es/ and http://www.cadcamcae.net/
[5] F.L Texeira and W C. Chew, "General closed-form PML constitutive linear media," IEEE Microw. Guid. Wave Lett., vol.8, no 6, pp 223–225, June 1998.
[6] Y. Tsuji and M. Koshiba, "Finite element method using port truncation by perfectly matched layer boundary conditions for optical waveguide discontinuity problems," J. Lightwave Technol., vol 20, no.3, pp.463–468, March 2002.
[7] H. Kobayashi and T. Wakabayashi, "Coupling characteristics ofmicrostrip lines through an elliptical slot," IEICE Trans Electron. (Japanese Edition), vol.J83-C, no.12, pp.1085–1092, Dec. 2000.
[8] Y. Hayashi, G. Mishima, K. Hirayama, and Y. Hayashi, "Simultaneous measurement of permittivity and permeability of lossy sheet using flanged rectangular waveguide," IEICE Trans. Electron. (Japanese Edition), vol.J85-C, no.9, pp 810–818, Sept. 2002.
[9] B.E. Little, S.T. Chu, H A. Haus, J. Foresi, and J.-P. Laine, "Microring resonator channel dropping filters," J. Lightwave Technol., vol.15, no.6, pp.998–1005, June 1997.
[10] K. Hirayama, K. Suzuki, and Y. Hayashi, "Finite element analysis of leaky wave in a dielectric ring resonator," IEICE Trans. Electron. (Japanese Edition), vol.J85-C, no.12, pp.1233–1235, Dec. 2002

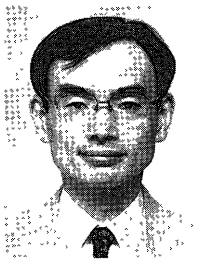

Koichi Hirayama was born in Shiranuka, Hokkaido, Japan, on September 8, 1961 He received the B.S., M.S., and Ph.D. degrees in electronic engineering from Hokkaido University, Sapporo, Japan, in 1984, 1986, and 1989, respectively. In 1989, he joined the Department of Electronic Engineering, Kushiro National College of Technology, Kushiro, Japan. In 1992, he became an Associate Professor of Electronic Engineering at Kitami Institute of Technology, Kitami, Japan. He has been interested in the analysis of propagation and scattering characteristics in electromagnetic and optical waveguides. Dr. Hirayama is a member of the Japan Society of Applied Physics and a senior member of the Institute of Electrical and Electronic Engineers (IEEE).

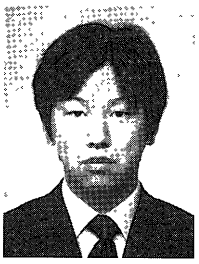

Naoto Kunieda was born in Asahikawa, Hokkaido, Japan, on April 28, 1979. He received the B.E. degree in electrical and electronic engineering from Kitami Institute of Technology, Kitami, Japan, in 2002, and is currently studying toward the M.E. degrees there. He has been interested in the analysis of the coupled microstrip lines via slots.

Yoshio Hayashi was born in Tokyo, Japan, on October 28, 1937. He received the B.E. degree in electrical engineering from Chiba University, Chiba, Japan, in 1961, and the M.E. and Ph D. degrees in electronics engineering from Hokkaido University, Sapporo, Japan, in 1965 and 1972, respectively. He served in the Japan Self-Defense Air Force from 1961 to 1969. He was a Visiting Scholar of Electrical Engineering at the University of Illinois, Urbana, from 1981 to 1982. Currently, he is a Professor of Electrical and Electronic Engineering at Kitami Institute of Technology, Kitami, Japan. He has been engaged in research on microwave field theory and electromagnetic wave problems Dr. Hayashi is a member of the Image Information and Television Engineers of Japan.

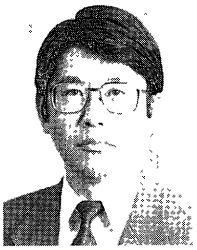

Masanori Koshiba was born in Sapporo, Japan, on November 23, 1948. He received the B.S., M S., and Ph D. degrees in electronic engineering from Hokkaido University, Sapporo, Japan, in 1971, 1973, and 1976, respectively In 1976, he joined the Department of Electronic Engineering, Kitami Institute of Technology, Kitami, Japan. From 1979 to 1987, he was an Associate Professor of Electronic Engineering at Hokkaido University, and in 1987, he became a Professor. He has been engaged in research on wave electronics, including microwaves, millimeter-waves, lightwaves, surface acoustic waves (SAW), magnetostatic waves (MSW), and electron waves, and computer-aided design and modeling of guided-wave devices using finite element method, boundary element method, beam propagation method, etc He is an author or coauthor of more than 200 research papers in English and of more than 100 research papers in Japanese both in refereed journals. He authored the books *Optical Waveguide Analysis* (New York: McGraw-Hill) and *Optical Waveguide Theory by the Finite Element Method* (Tokyo/Dordrecht. KTK Scientific/Kluwer), and coauthored the books *Analysis Methods for Electromagnetic Wave Problems* (Norwood, MA. Artech House), *Ultrafast and Ultra-parallel Optoelectronics* (New York: Wiley), and *Finite Element Software for Microwave Engineering* (New York. Wiley). From 1999 to 2000, he served as a President of the IEICE, Electronics Society, and since 2000, he has served on the Board of Directors of the Applied Computational Electromagnetics Society (ACES) Dr Koshiba is a member of the Institute of Electrical Engineers of Japan, the Institute of Image Information and Television Engineers of Japan, the Japan Society for Simulation Technology, the Japan Society for Computational Methods in Engineering, Japan Society of Applied Electromagnetics and Mechanics, the Japan Society for Computational Engineering and Science, and ACES, and a Fellow of the Institute of Electrical and Electronic Engineers (IEEE). In 1987, 1997, and 1999, he received the Excellent Paper Awards from the IEICE, and in 1998, he received the Electronics-Society Award from the IEICE.